Quantum Algorithms for Quantum Many-Body Systems

Dean Lee
Facility for Rare Isotope Beams
Michigan State University

NP-AMO QIS Workshop
University of Massachusetts Boston
January 13, 2024

Outline

Nuclear lattice effective field theory

What problems are beyond classical computing?

Rodeo algorithm

Controlled reversal gates

Multi-state rodeo algorithm

Fusion method

Quantum evaporative cooling

Wavefunction matching

Adiabatic perturbation theory

Nuclear lattice simulations on quantum computers

Summary

Lattice effective field theory

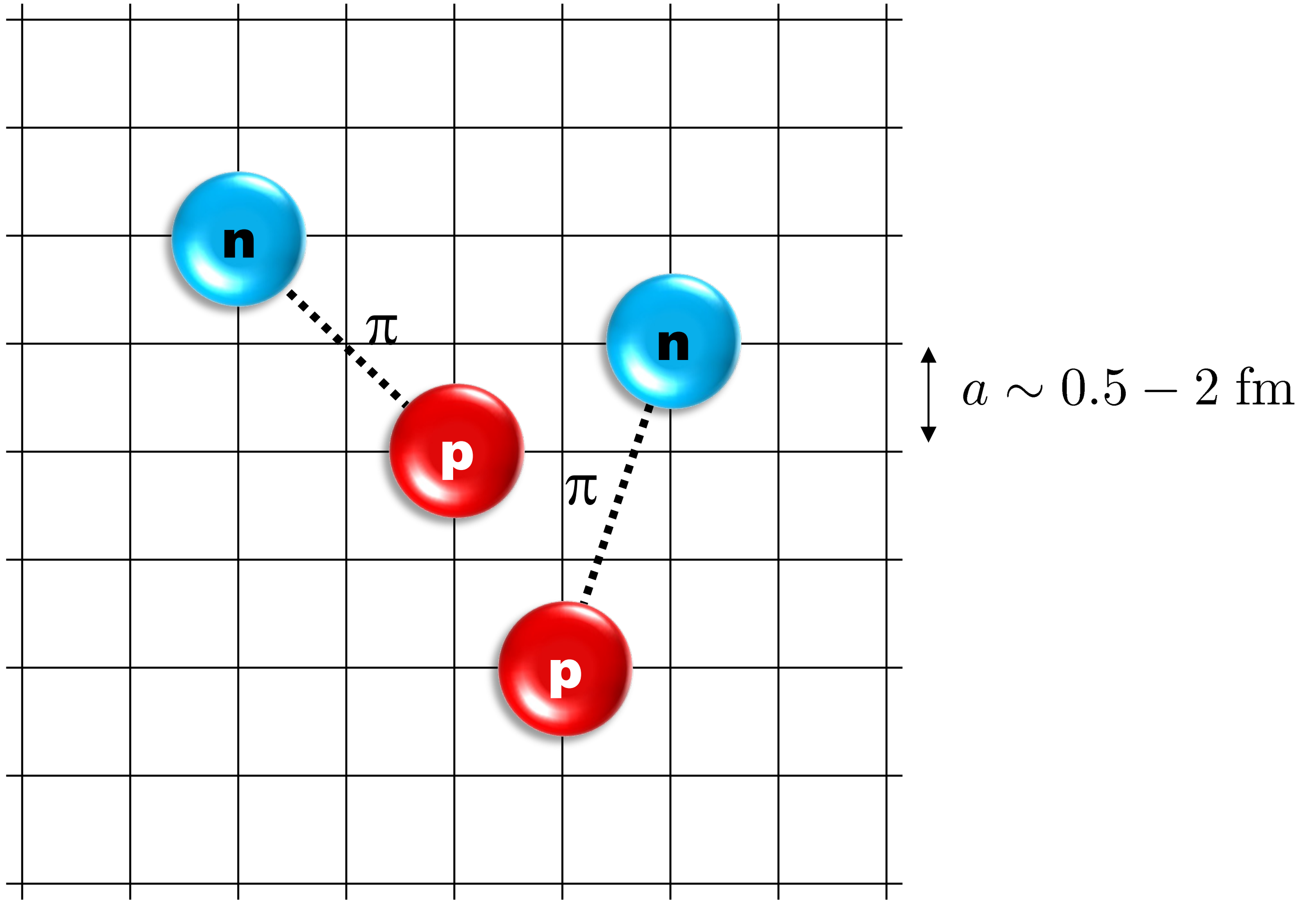

D.L, Prog. Part. Nucl. Phys. 63 117-154 (2009); D.L., arXiv:2501.03303

Lähde, Meißner, Nuclear Lattice Effective Field Theory (2019), Springer

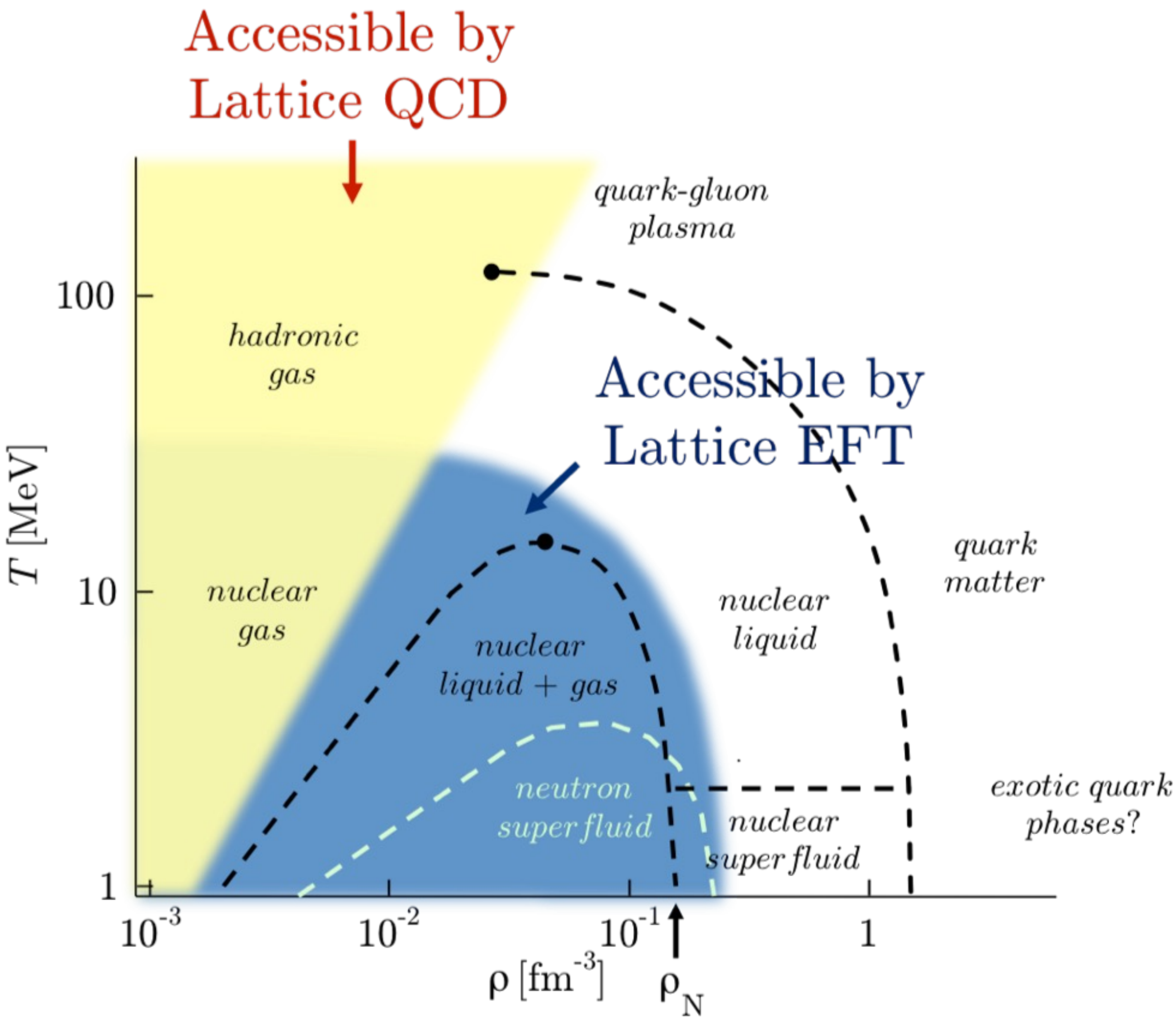
Accessible by
Lattice QCD
quark-gluon
plasma
hadronic
gas
Accessible by
Lattice EFT
nuclear
gas
nuclear
liquid + gas
nuclear
liquid
quark
matter
neutron
superfluid
nuclear
superfluid
exotic quark
phases?
T [MeV]
100
10
1
10^{-3}
10^{-2}
10^{-1}
1
ρ [fm^{-3}]
ρ_N

Chiral effective field theory

Construct the effective potential order by order

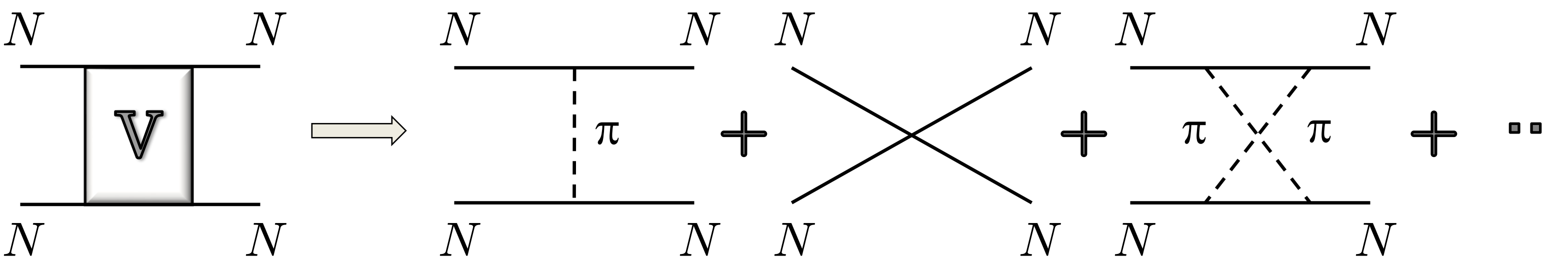

V^{OPEP} Contact interactions V^{TPEP}

Leading order (LO) Next-to-leading order (NLO)

$a = 1.315\,\mathrm{fm}$

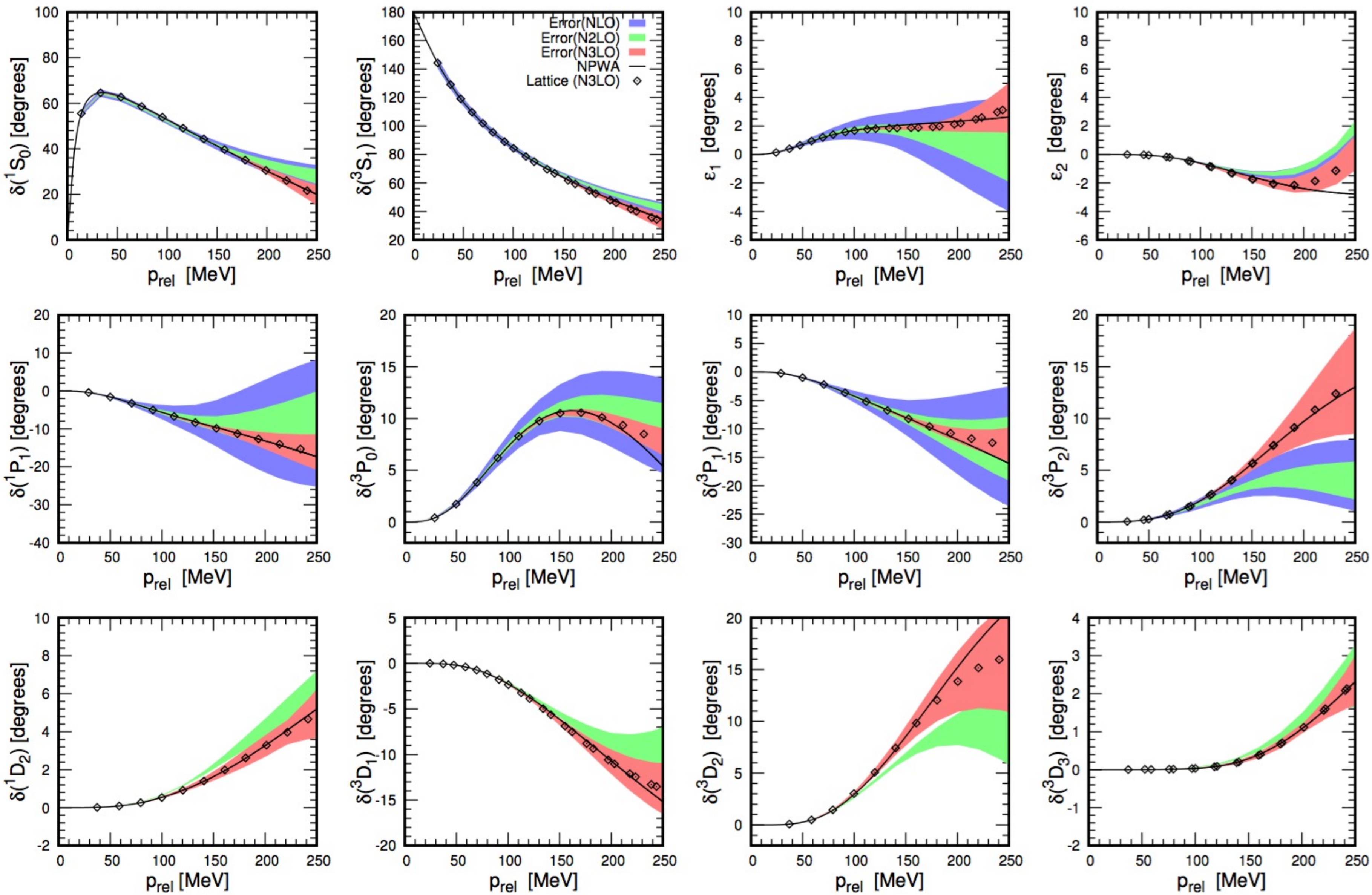

Li, Elhatisari, Epelbaum, D.L., Lu, Meißner, PRC 98, 044002 (2018)

Binding energies

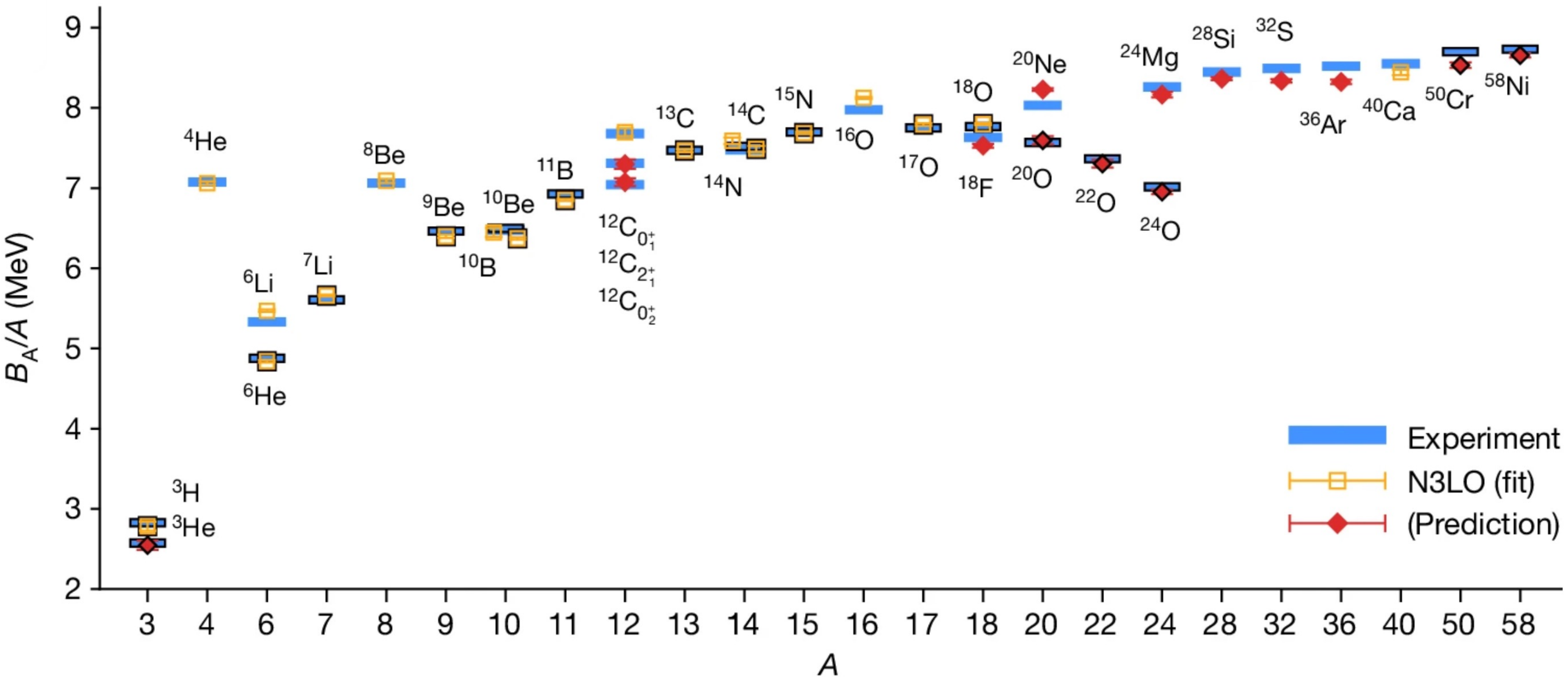

Elhatisari, Bovermann, Ma, Epelbaum, Frame, Hildenbrand, Krebs, Lähde, D.L., Li, Lu, M. Kim, Y. Kim, Meißner, Rupak, Shen, Song, Stellin, Nature 630, 59 (2024)

Charge radii

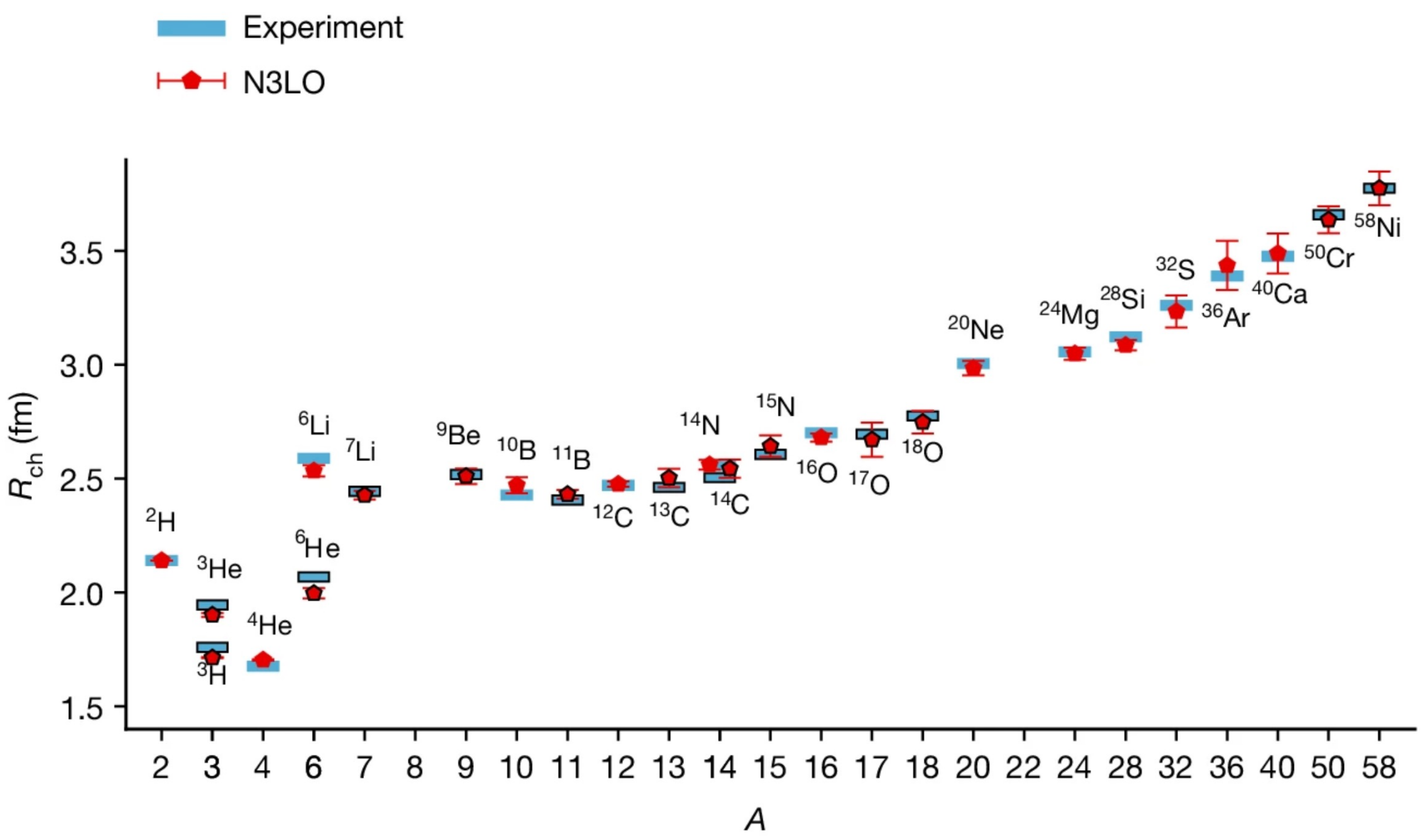

Elhatisari, Bovermann, Ma, Epelbaum, Frame, Hildenbrand, Krebs, Lähde, D.L., Li, Lu, M. Kim, Y. Kim, Meißner, Rupak, Shen, Song, Stellin, Nature 630, 59 (2024)

Emergent geometry and duality of ^{12}C

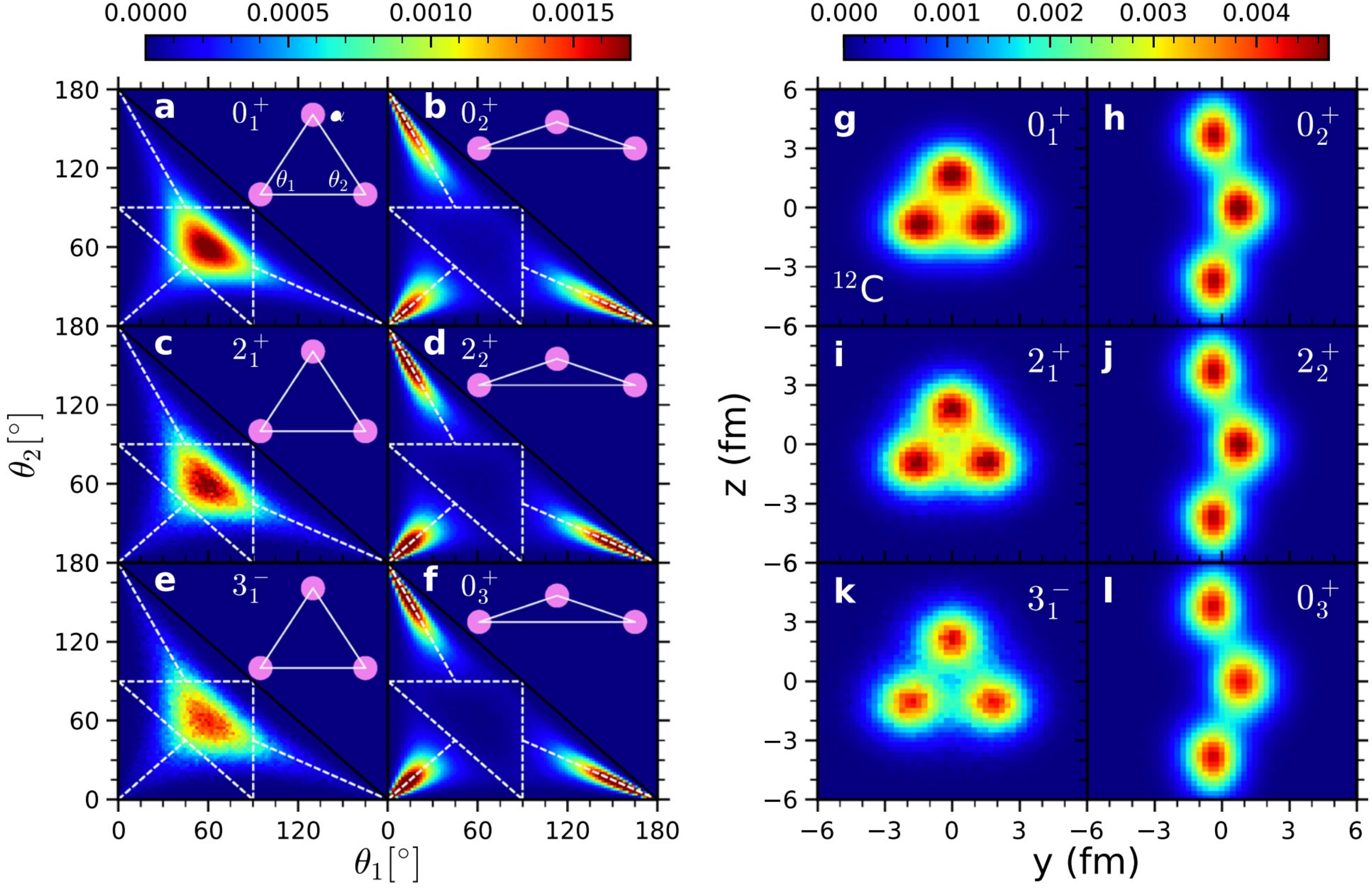

Shen, Elhatisari, Lähde, D.L., Lu, Meißner, Nature Commun. 14, 2777 (2023)

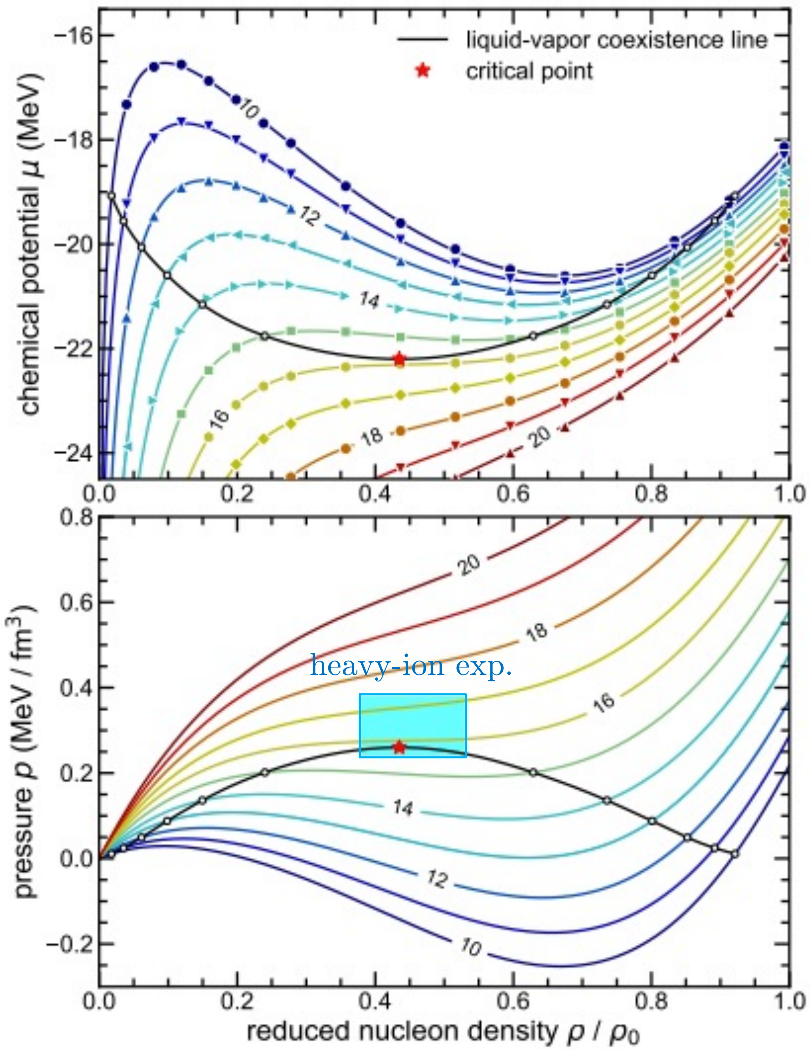

Liquid-vapor critical point

$$T_c = 15.80(0.32)(1.60)\,\mathrm{MeV}$$
$$\rho_c = 0.089(04)(18)\,\mathrm{fm}^{-3}$$
$$\mu_c = -22.20(0.44)(2.20)\,\mathrm{MeV}$$
$$P_c = 0.260(05)(30)\,\mathrm{MeV\ fm}^{-3}$$

Lu, Li, Elhatisari, D.L., Drut, Lähde, Epelbaum, Meißner, Phys. Rev. Lett. 125, 192502 (2020)

What problems are beyond classical computing?

$$\exp(-iHt) \rightarrow \exp(-H\tau)$$

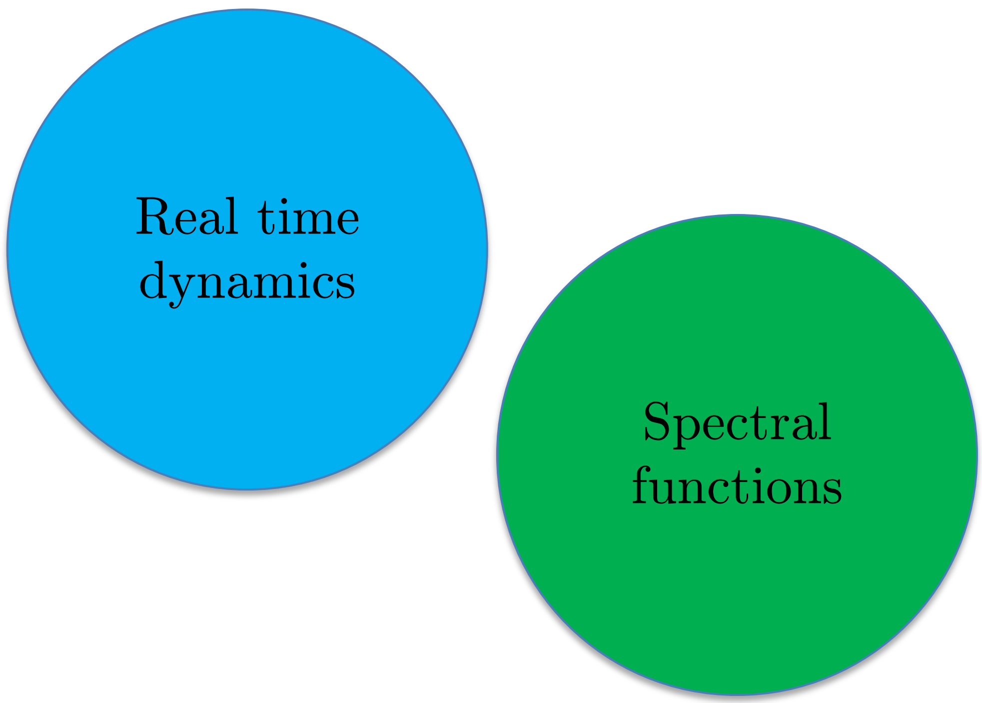

Rodeo algorithm

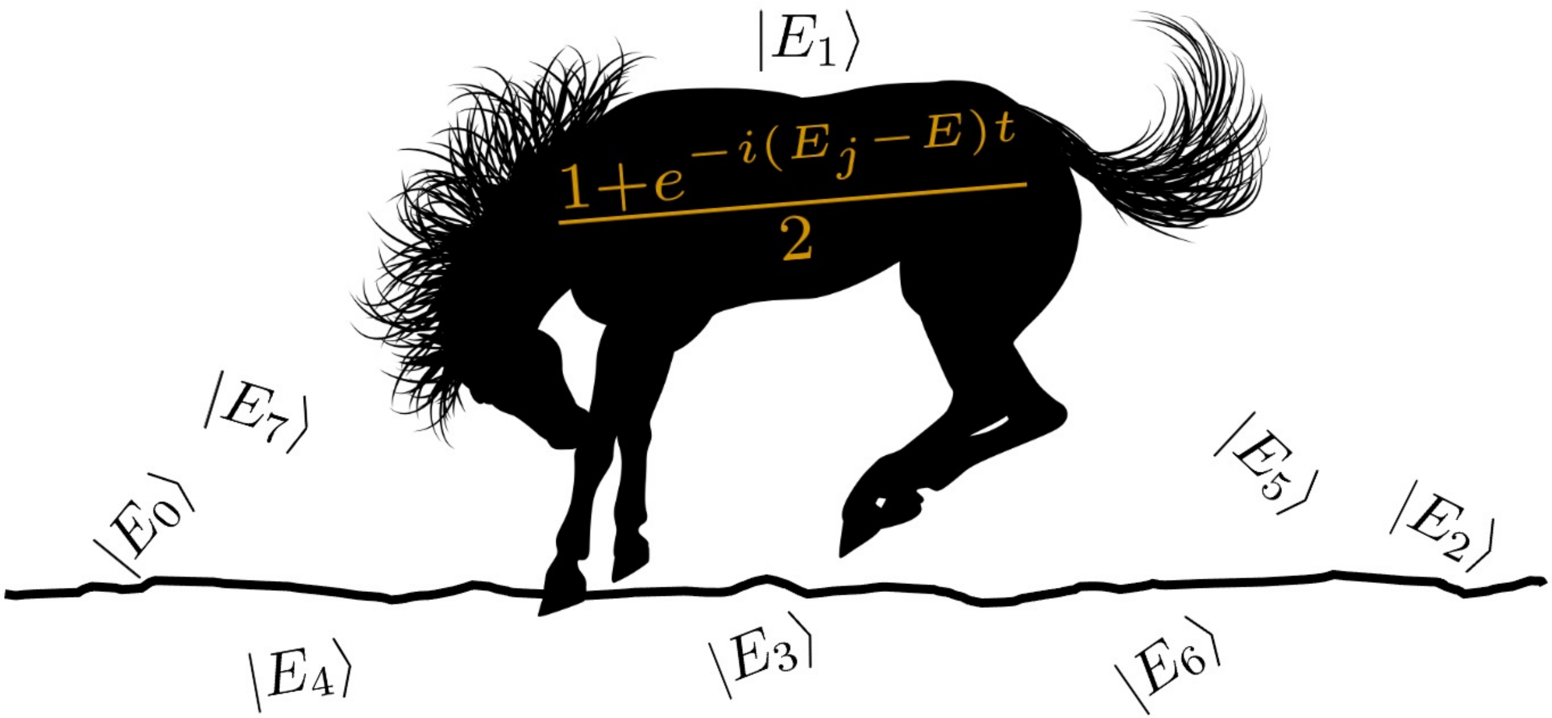

Choi, D.L., Bonitati, Qian, Watkins, PRL 127, 040505 (2021)

Consider a single qubit and a Hadamard gate

$$U = \begin{bmatrix} \frac{1}{\sqrt{2}} & \frac{1}{\sqrt{2}} \\ \frac{1}{\sqrt{2}} & -\frac{1}{\sqrt{2}} \end{bmatrix} = U^\dagger = U^{-1}$$

Consider another unitary operation that is a diagonal phase rotation

$$R(E_{\text{obj}}, E, t) = \begin{bmatrix} 1 & 0 \\ 0 & e^{-it(E_{\text{obj}} - E)} \end{bmatrix}$$

We then have

$$U^\dagger R(E_{\text{obj}}, E, t) U = \begin{bmatrix} \frac{1}{2} + \frac{1}{2} e^{-it(E_{\text{obj}} - E)} & \frac{1}{2} - \frac{1}{2} e^{-it(E_{\text{obj}} - E)} \\ \frac{1}{2} - \frac{1}{2} e^{-it(E_{\text{obj}} - E)} & \frac{1}{2} + \frac{1}{2} e^{-it(E_{\text{obj}} - E)} \end{bmatrix}$$

Let us now start in the $\begin{bmatrix} 0 \\ 1 \end{bmatrix}$ state and perform these unitary operations

$$U^\dagger R(E_{\text{obj}}, E, t) U \begin{bmatrix} 0 \\ 1 \end{bmatrix} = \begin{bmatrix} \frac{1}{2} - \frac{1}{2} e^{-it(E_{\text{obj}} - E)} \\ \frac{1}{2} + \frac{1}{2} e^{-it(E_{\text{obj}} - E)} \end{bmatrix}$$

and then project back to the $\begin{bmatrix} 0 \\ 1 \end{bmatrix}$ state

$$\begin{bmatrix} 0 & 0 \\ 0 & 1 \end{bmatrix} U^\dagger R(E_{\text{obj}}, E, t) U \begin{bmatrix} 0 \\ 1 \end{bmatrix} = \begin{bmatrix} 0 \\ \frac{1}{2} + \frac{1}{2} e^{-it(E_{\text{obj}} - E)} \end{bmatrix}$$

This projection is done via quantum measurement and the success probability is

$$P(E_{\text{obj}}, E, t) = \left| \frac{1}{2} + \frac{1}{2} e^{-it(E_{\text{obj}} - E)} \right|^2 = \cos^2 \left[\frac{t(E_{\text{obj}} - E)}{2} \right]$$

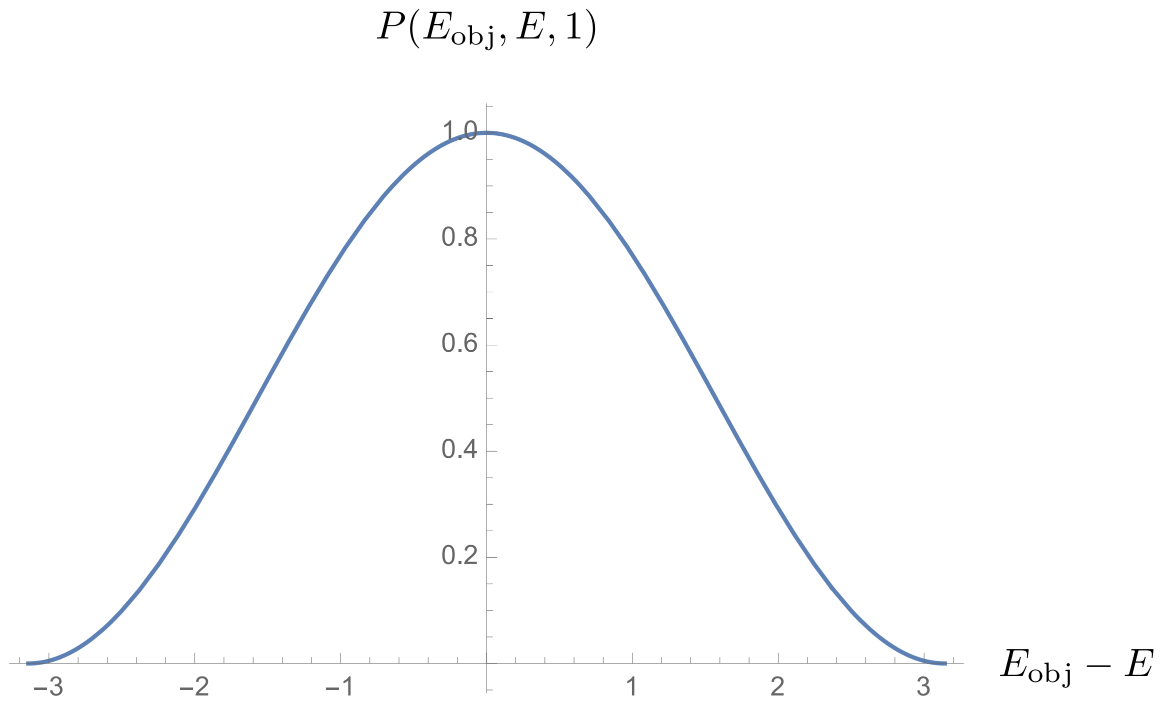
$P(E_{\rm obj}, E, 1)$
1.0
0.8
0.6
0.4
0.2
−3
−2
−1
1
2
3
$E_{\rm obj} - E$

$P(E_{\mathrm{obj}}, E, 14.2023)$

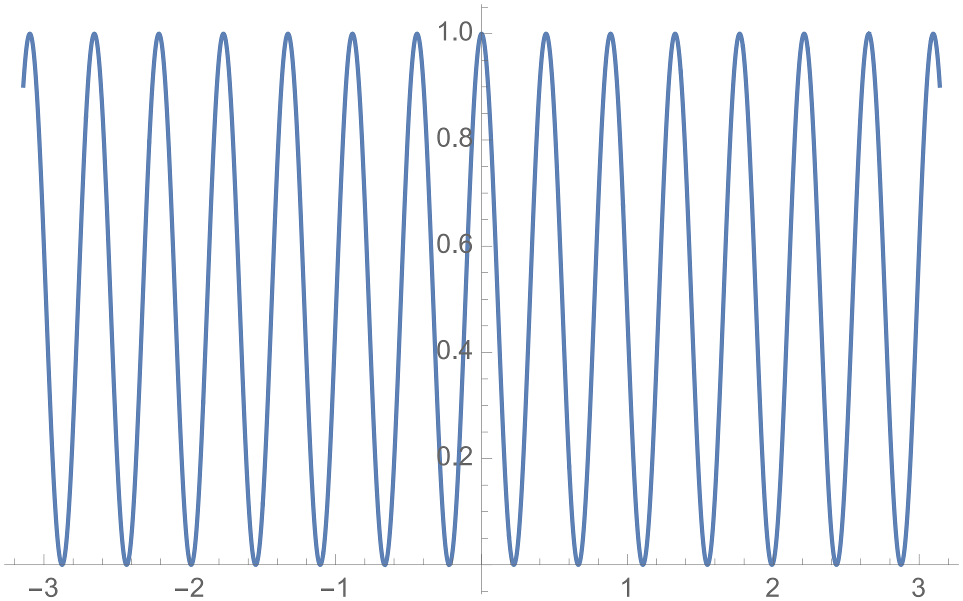

$$\prod_{k=1}^{5} P(E_{\rm obj}, E, t_k) \qquad |t_k| < 50$$

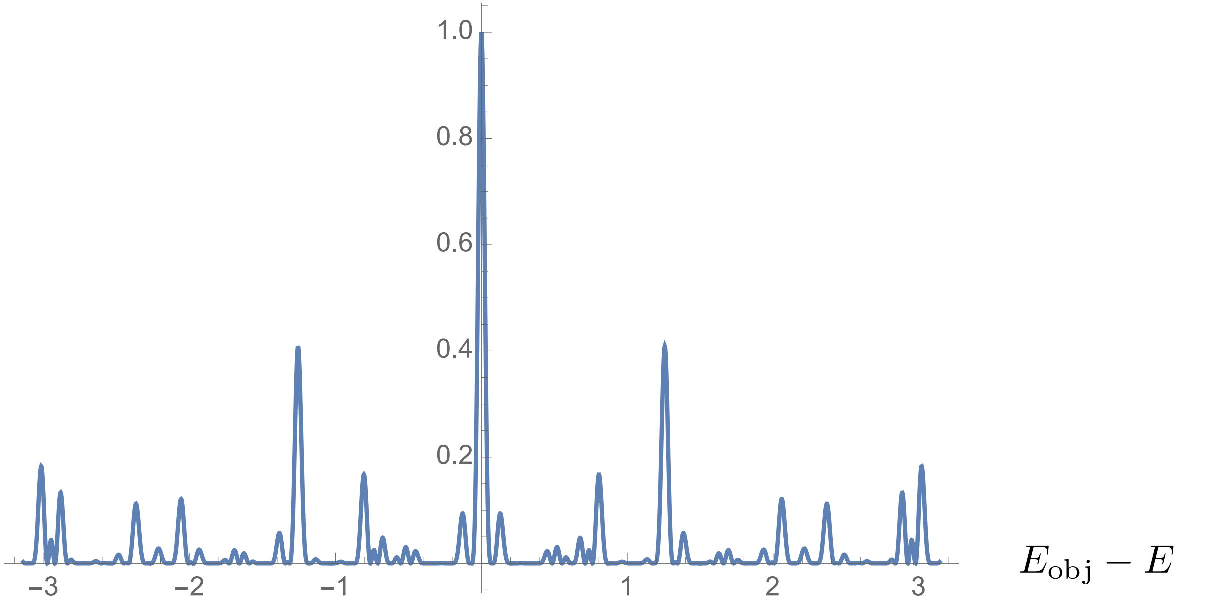

$$\prod_{k=1}^{10} P(E_{\mathrm{obj}}, E, t_k) \qquad |t_k| < 50$$

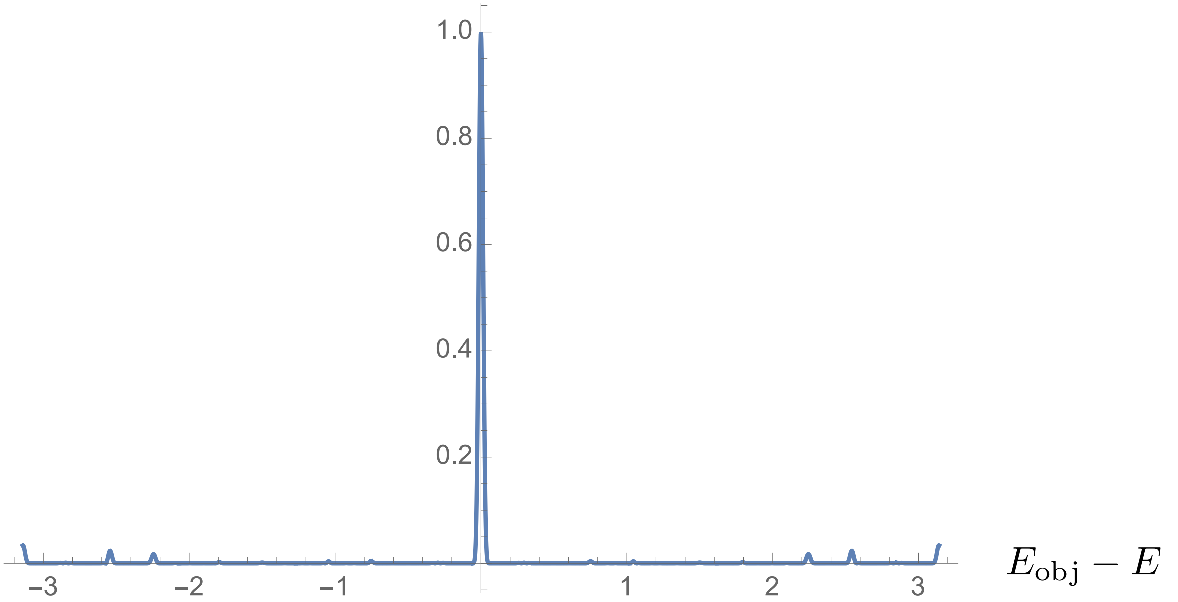

Let us couple this qubit, which we call the "arena" or "ancilla" qubit, to another system that we call the "object". We also promote the 2 x 2 matrices to become 2 x 2 matrices of operators acting on the object.

$$\begin{bmatrix} \frac{1}{\sqrt{2}} & \frac{1}{\sqrt{2}} \\ \frac{1}{\sqrt{2}} & -\frac{1}{\sqrt{2}} \end{bmatrix} \to \begin{bmatrix} \frac{\hat{I}}{\sqrt{2}} & \frac{\hat{I}}{\sqrt{2}} \\ \frac{\hat{I}}{\sqrt{2}} & -\frac{\hat{I}}{\sqrt{2}} \end{bmatrix}$$

$$\begin{bmatrix} 1 & 0 \\ 0 & e^{-it(E_{\mathrm{obj}}-E)} \end{bmatrix} \to \begin{bmatrix} \hat{I} & 0 \\ 0 & e^{-it(\hat{H}_{\mathrm{obj}}-E)} \end{bmatrix}$$

We then consider the same combination

$$\begin{bmatrix} \frac{\hat{I}}{\sqrt{2}} & \frac{\hat{I}}{\sqrt{2}} \\ \frac{\hat{I}}{\sqrt{2}} & -\frac{\hat{I}}{\sqrt{2}} \end{bmatrix} \begin{bmatrix} \hat{I} & 0 \\ 0 & e^{-it(\hat{H}_{\mathrm{obj}}-E)} \end{bmatrix} \begin{bmatrix} \frac{\hat{I}}{\sqrt{2}} & \frac{\hat{I}}{\sqrt{2}} \\ \frac{\hat{I}}{\sqrt{2}} & -\frac{\hat{I}}{\sqrt{2}} \end{bmatrix}$$

We start from the state $\begin{bmatrix} 0 \\ |\psi_{\text{init}}\rangle \end{bmatrix}$ and we perform the operations and then measure if the arena qubit is in the $\begin{bmatrix} 0 \\ 1 \end{bmatrix}$ state

$$\begin{bmatrix} 0 & 0 \\ 0 & \hat{I} \end{bmatrix} \begin{bmatrix} \frac{\hat{I}}{\sqrt{2}} & \frac{\hat{I}}{\sqrt{2}} \\ \frac{\hat{I}}{\sqrt{2}} & -\frac{\hat{I}}{\sqrt{2}} \end{bmatrix} \begin{bmatrix} \hat{I} & 0 \\ 0 & e^{-it(\hat{H}_{\text{obj}}-E)} \end{bmatrix} \begin{bmatrix} \frac{\hat{I}}{\sqrt{2}} & \frac{\hat{I}}{\sqrt{2}} \\ \frac{\hat{I}}{\sqrt{2}} & -\frac{\hat{I}}{\sqrt{2}} \end{bmatrix} \begin{bmatrix} 0 \\ |\psi_{\text{init}}\rangle \end{bmatrix} = \begin{bmatrix} 0 \\ [\frac{1}{2} + \frac{1}{2} e^{-it(\hat{H}_{\text{obj}}-E)}] \, |\psi_{\text{init}}\rangle \end{bmatrix}$$

By repeated successful measurements with random values of t, we reduce the spectral weight of eigenvectors with energies that do not match E.

The convergence is exponential. For N cycles of the rodeo algorithm, the suppression factor for undesired energy states is $1/4^N$.

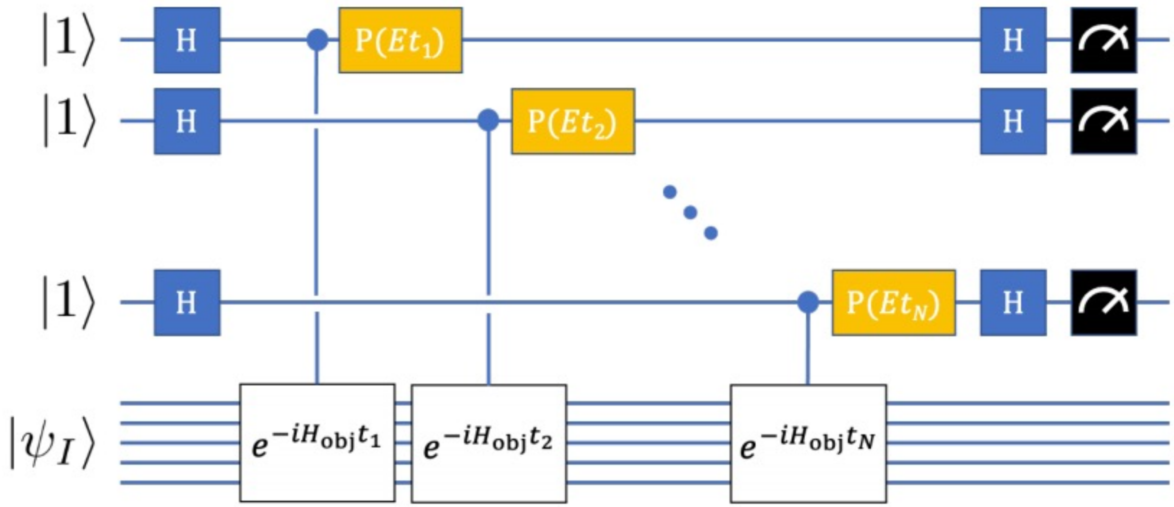

FIG. 1. (color online) **Circuit diagram for the rodeo algorithm.** The object system starts in an arbitrary state $|\psi_I\rangle$. Each of the arena qubits are initialized in the state $|1\rangle$ and operated on by a Hadamard gate H. We use each arena qubit $n = 1, \cdots, N$ for the controlled time evolution of the object Hamiltonian, H_{obj}, for time t_n. This is followed by a phase rotation $\text{P}(Et_n)$ on arena qubit n, another Hadamard gate H, and then measurement.

Choi, D.L., Bonitati, Qian, Watkins, PRL 127, 040505 (2021)

Initial-state spectral function and state preparation. The example shown below is for a 1D Heisenberg chain with ten sites, antiferromagnetic interactions, and uniform magnetic field.

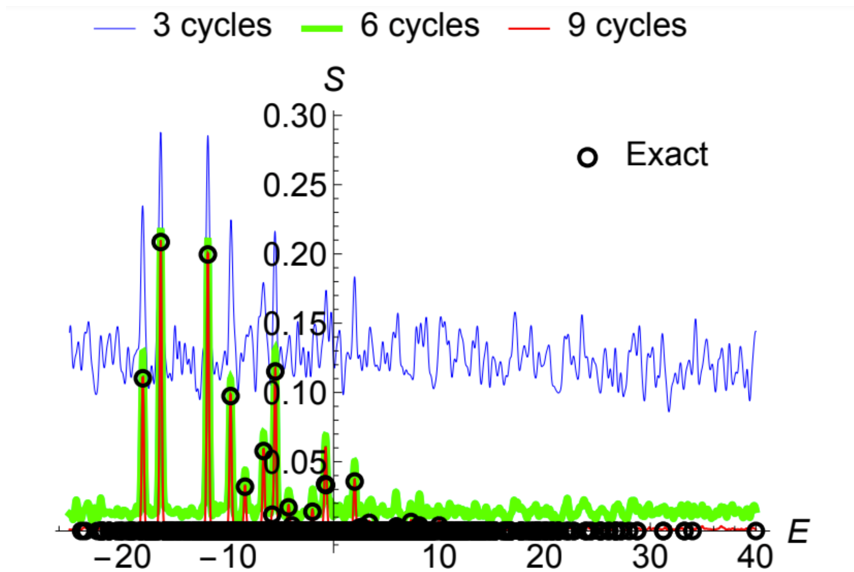

FIG. 4. (color online) **Initial-state spectral function for the Heisenberg model.** We plot the initial-state spectral function using the rodeo algorithm for the Heisenberg spin chain with 3 (thin blue line), 6 (thick green line), and 9 (medium red line) cycles. We have averaged over 20 sets of Gaussian random values for t_n with $t_{\mathrm{RMS}} = 5$. For comparison, we also show the exact initial-state spectral function with black open circles.

$$|\psi_{\mathrm{init}}\rangle = |0101010101\rangle$$

Controlled reversal gates

A reversal gate, R, is a product of single qubit gates that anticommutes with some subset of the terms in a Hamiltonian.

$$RH = -HR$$

We note that

$$Re^{-iHt}R = e^{+iHt}$$

Let C_R be the controlled reversal gate that performs R if the ancilla qubit is in the 1 state and does nothing if the ancilla qubit is in the 0 state.

C_R toggles the flow of time back and forth. With C_R we can reduce the number of gates needed for state preparation.

Our Hamiltonian has the form

$$H_{\text{obj}} = c_1 X_1 \otimes Z_2 + c_2 Z_1 \otimes X_2$$

$$c_1 = 2.5,\ c_2 = 1.5$$

The time evolution of the Hamiltonian can be expressed with this simple circuit

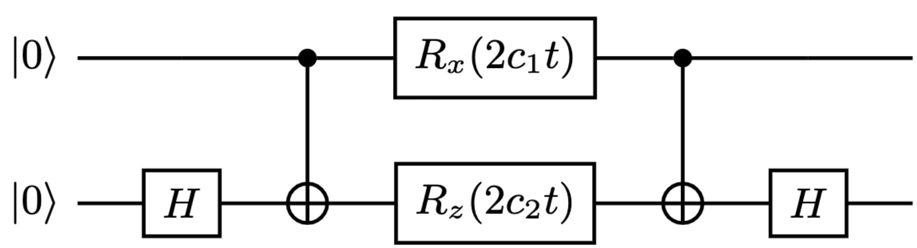

Using controlled reversal gates, one cycle of the rodeo algorithm is implemented as

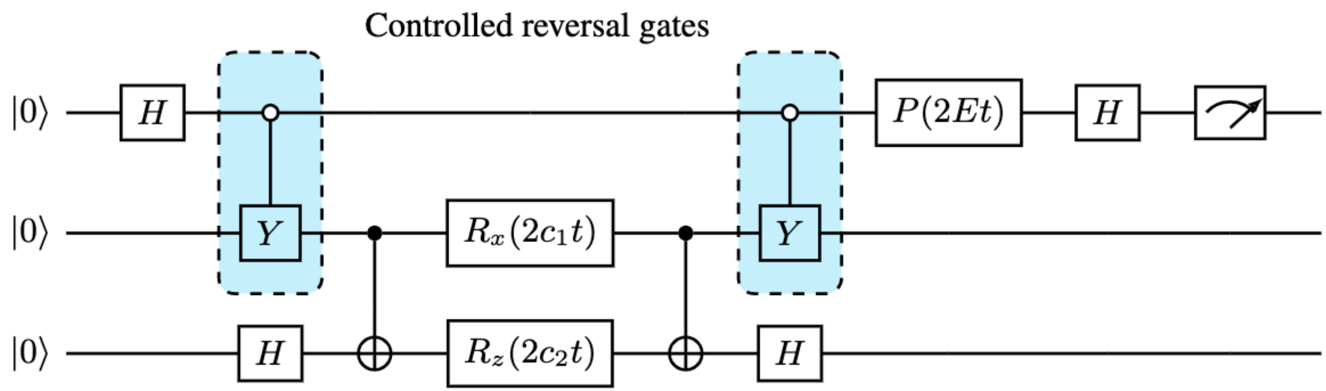

The controlled reversal gates provide a fivefold reduction in the number of gates. The comparison is made with respect to Qiskit-transpiled code without controlled reversal gates.

Bee-Lindgren, Qian, DeCross, Brown, Gilbreth, Watkins, Zhang, D.L., arXiv:2208.13557

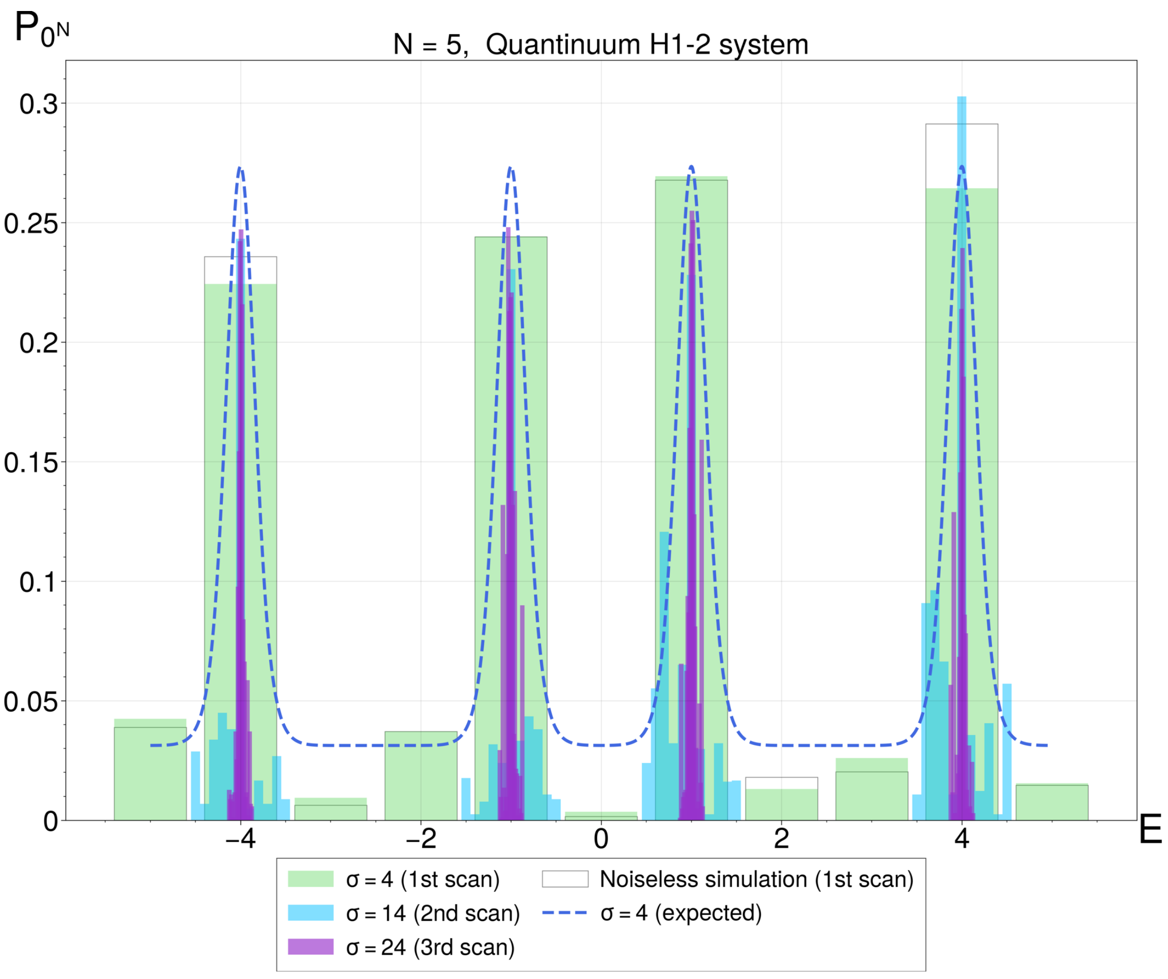

N = 5, Quantinuum H1-2 system
P0N
0.3
0.25
0.2
0.15
0.1
0.05
0
−4
−2
0
2
4
E
σ = 4 (1st scan)
σ = 14 (2nd scan)
σ = 24 (3rd scan)
Noiseless simulation (1st scan)
σ = 4 (expected)

	Exact	IBM Perth Three Cycles	IBM Perth Five Cycles	Quantinuum H1-2 Five Cycles
$\vert\psi_0\rangle$	-4.0000	-4.0022(49)	-4.0006(42)	-3.9982(21)
$\vert\psi_1\rangle$	-1.0000	-0.9829(56)	-0.9927(40)	-1.0083(39)
$\vert\psi_2\rangle$	1.0000	1.0007(26)	1.0008(19)	1.0028(22)
$\vert\psi_3\rangle$	4.0000	4.0093(84)	3.9982(25)	4.0036(17)

Multi-state rodeo algorithm

We can prepare an arbitrary linear combination of two eigenvectors with two different energies.

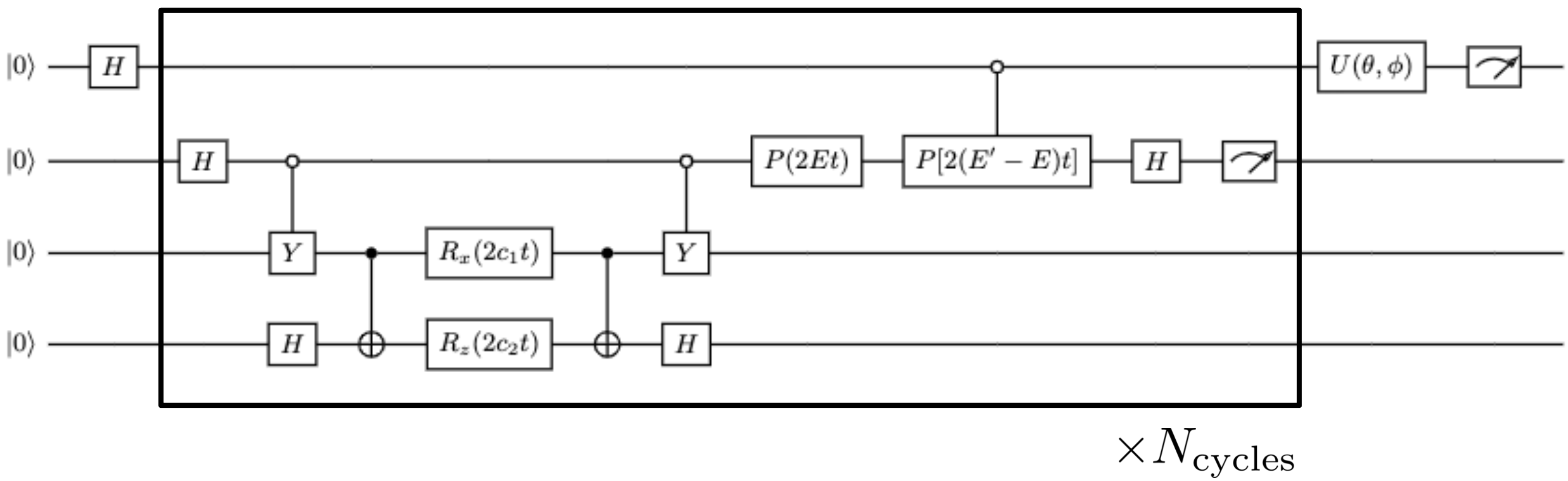

Bee-Lindgren, Qian, *et al.*, work in progress

This allows us to create the general superposition state

$$|\theta, \phi\rangle = \cos(\theta/2)\,|E\rangle + e^{i\phi}\sin(\theta/2)\,|E'\rangle$$

We can now measure the expectation value of any observable O

$$\begin{aligned}\langle\theta, \phi|O|\theta, \phi\rangle = \cos^2(\theta/2)\,\langle E|O|E\rangle + \sin^2(\theta/2)\,\langle E'|O|E'\rangle \\ + \Re[e^{i\phi}\sin(\theta)\,\langle E|O|E'\rangle]\end{aligned}$$

From this we can extract the transition matrix element

$$\langle E|O|E'\rangle$$

Fusion method

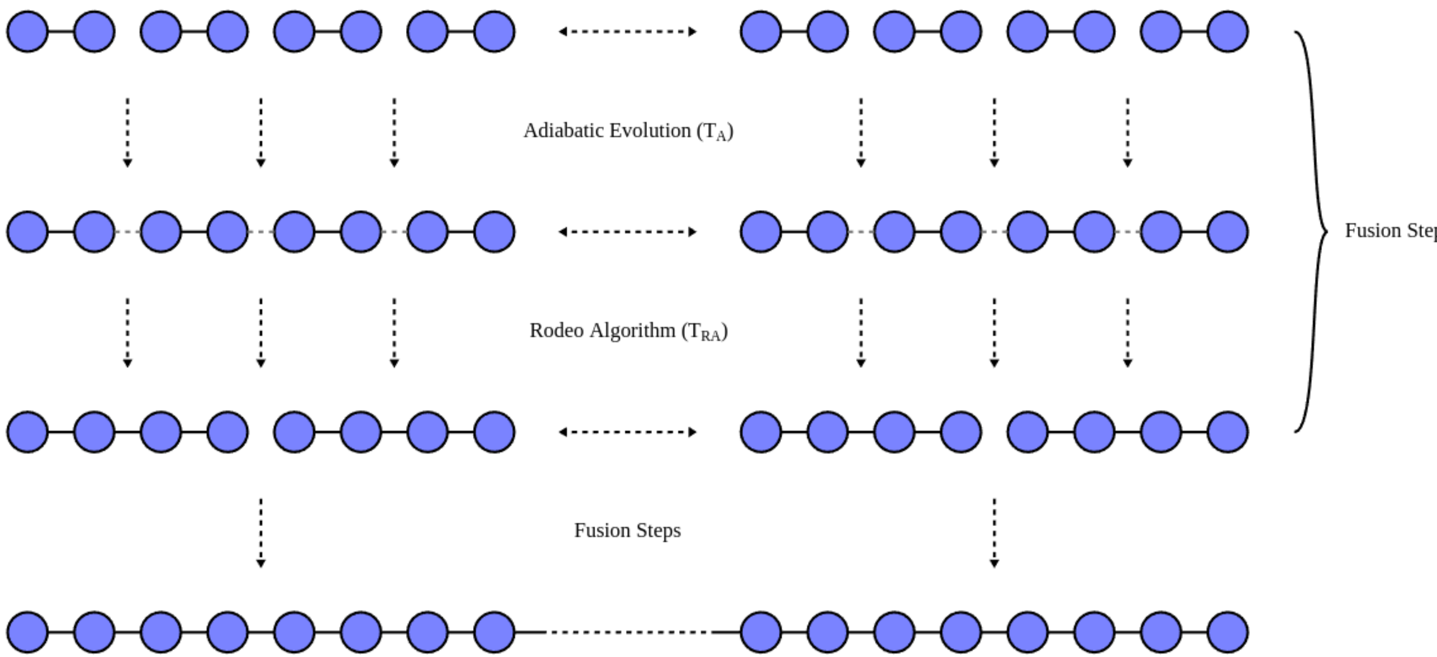

Figure by M. Patkowski

Patkowski, Ayyildiz, Hunt, D.L., work in progress

Quantum evaporative cooling

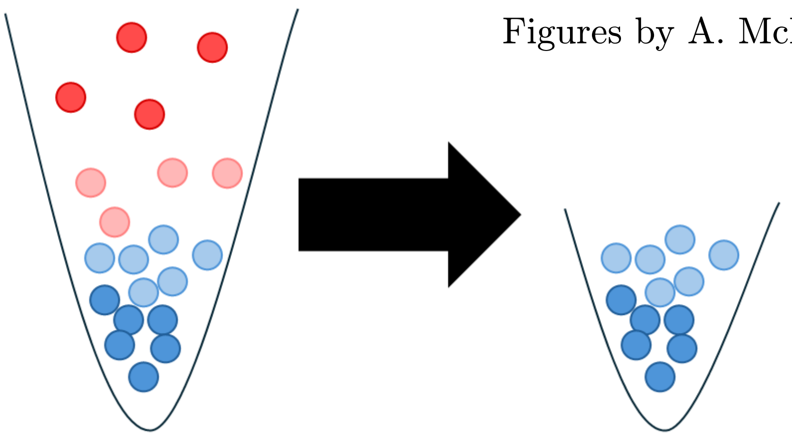

Figures by A. McRae

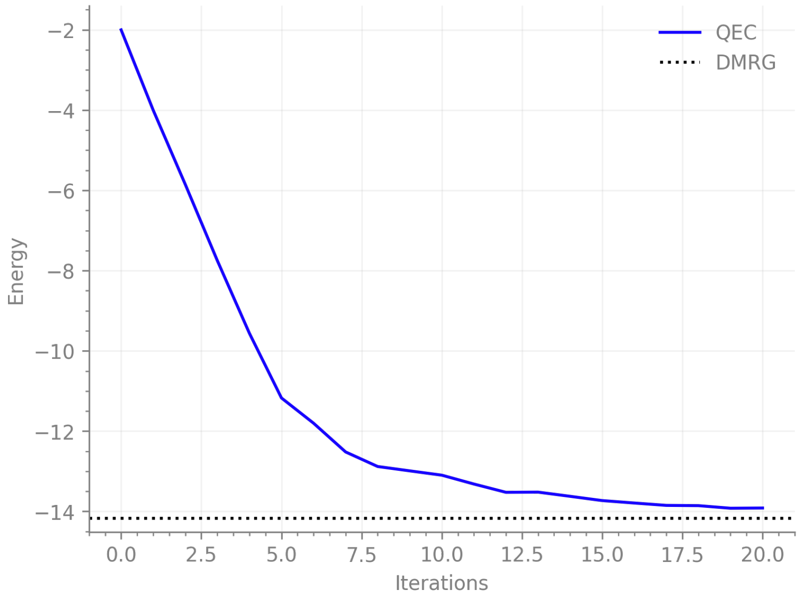

Projected cooling algorithm

Phys. Lett. B 807, 10 (2020), D.L., Bonitati, Given, Hicks, Li, Lu, Rai, Sarkar, Watkins

McRae, Hjorth-Jensen, D.L., work in progress

Wavefunction matching

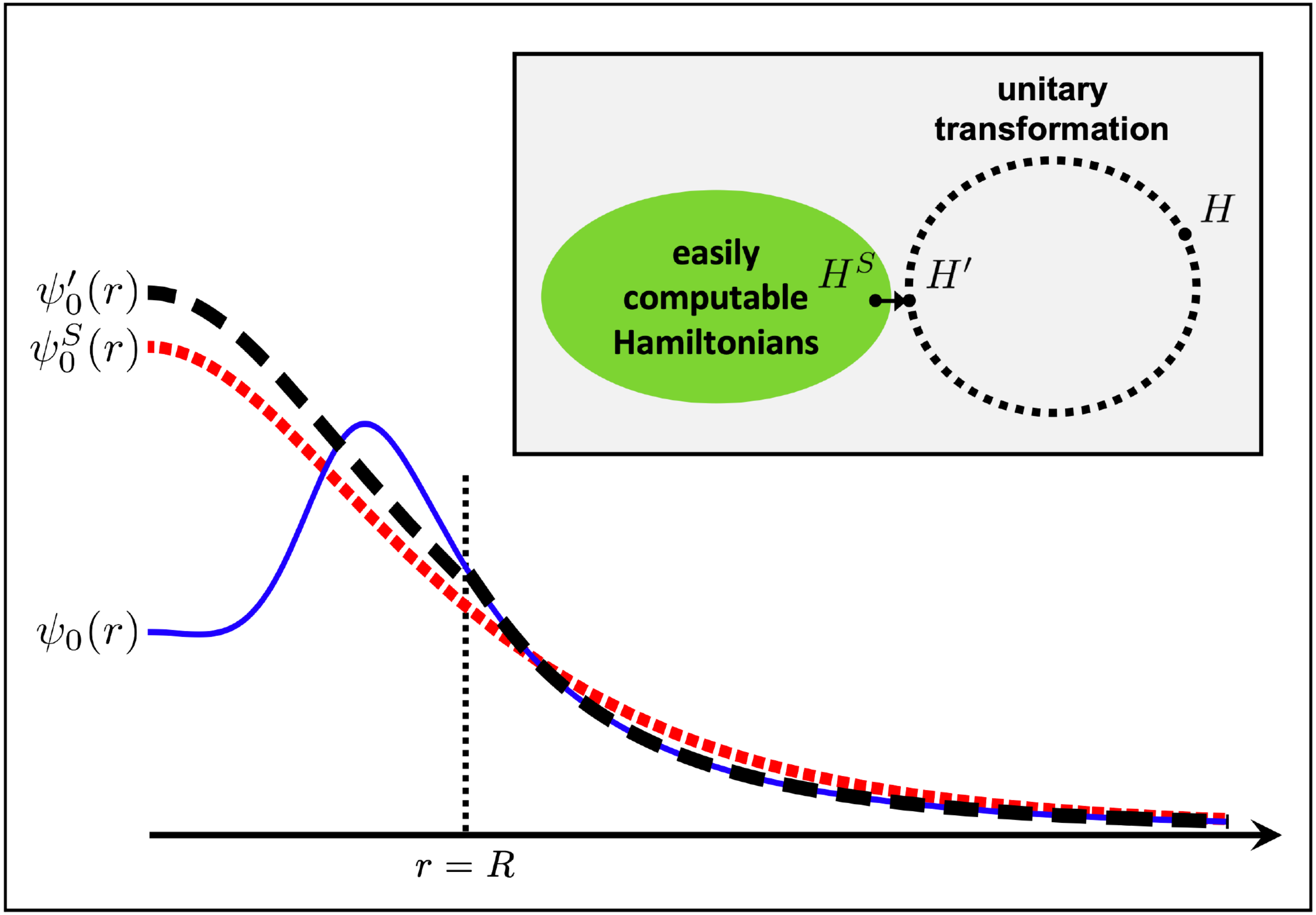

Elhatisari, Bovermann, Ma, Epelbaum, Frame, Hildenbrand, Krebs, Lähde, D.L., Li, Lu, M. Kim, Y. Kim, Meißner, Rupak, Shen, Song, Stellin, Nature 630, 59 (2024)

Adiabatic perturbation theory

$$H = H_0 + H_1$$

$$H_1(t) = f(t)H_1 \quad \begin{cases} f(0) = 0, f'(0) = 0, \cdots \\ f(t_F) = 1, f'(t_F) = 0, \cdots \end{cases}$$

$$T\exp[-i\int_0^{t_F} dt(H_0 + H_1(t))]$$
$$= \sum_k \left[\int_0^{t_F} dt_1 \cdots \int_{t_{k-1}}^{t_F} dt_k\right] e^{-iH_0(t_F - t_k)} H_1(t_k) e^{-iH_0(t_k - t_{k-1})} \cdots H_1(t_1) e^{-iH_0 t_1}$$

Cariello, Given, Hjorth-Jensen, D.L., work in progress

Nuclear lattice simulations on quantum computers

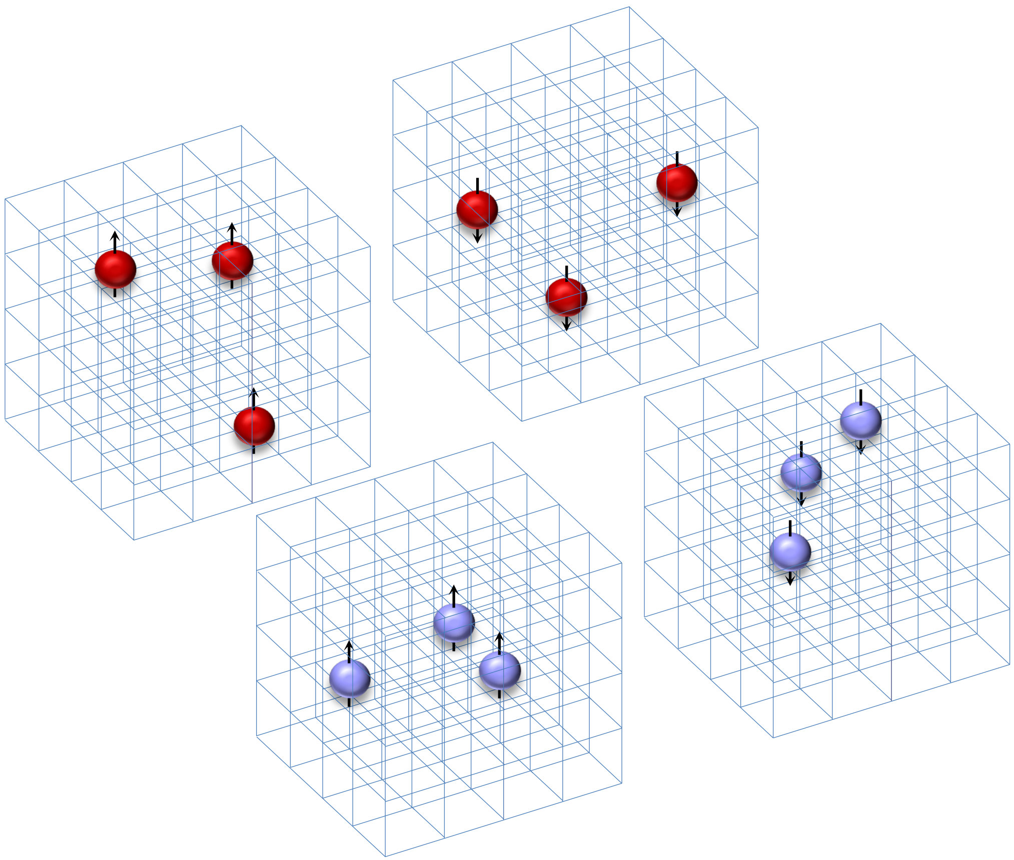

Summary

We introduced nuclear lattice effective field theory and discussed the possibility of future calculations of spectral functions and real time dynamics on quantum computers. We then discussed the rodeo algorithm and introduced the concept of controlled reversal gates for reducing circuit depth. We showed some applications of the rodeo algorithm on real quantum devices and considered the multi-state rodeo algorithm for preparing arbitrary linear combinations of energy eigenstates in order to compute transition matrix elements. We briefly introduced the fusion method, quantum evaporative cooling, wavefunction matching, and adiabatic perturbation theory. We concluded with an outlook on future prospects for nuclear lattice simulations on quantum computers.